
Article:
Melling, G.E., Flannery, S.E., Abidin, S.A. et al. (13 more authors) (2018) A miRNA-145/TGF-β1 Negative Feedback Loop Regulates the Cancer-Associated Fibroblast Phenotype. Carcinogenesis, 39 (6). pp. 798-807. ISSN 0143-3334

https://doi.org/10.1093/carcin/bgy032

A miRNA-145/TGF-β1 negative feedback loop regulates the cancer-associated fibroblast phenotype

Melling GE[1], Flannery SE[1], Abidin SA[1], Clemmens H[1], Prajapati P[1], Hinsley EE[1], Hunt S[1] Catto JWF[2], Coletta RD[3], Mellone M[4], Thomas GJ[4], Parkinson EK[5], Prime SS[5], Paterson IC[6], Buttle DJ[7] and Lambert DW[1,8*]

[1]School of Clinical Dentistry, University of Sheffield, S10 2TA, United Kingdom
[2]Unit of Academic Urology, University of Sheffield, S10 2RX, UK
[3]Department of Oral Diagnosis, School of Dentistry, University of Campinas, Piracicaba-SP, Brazil
[4]Faculty of Medicine Cancer Sciences Unit, Southampton University, Somers Building, MP 824 Tremona Road Southampton SO16 6YD, UK
[5]Centre for Immunobiology and Regenerative Medicine, Institute of Dentistry, Barts and the London School of Medicine and Dentistry, Queen Mary University of London, Turner Street, London E1 2AD, UK
[6]Department of Oral Biology and Biomedical Sciences and Oral Cancer Research and Coordinating Centre, Faculty of Dentistry, University of Malaya, 50603 Kuala Lumpur, Malaysia
[7]Department of Infection and Immunity and Cardiovascular Disease, University of Sheffield, S10 2RS, UK
[8]Sheffield Institute for Nucleic Acids, University of Sheffield, S102TA, UK

*Address for correspondence: Dr D W Lambert, School of Clinical Dentistry, University of Sheffield, Sheffield, S10 2TA, United Kingdom
d.w.lambert@sheffield.ac.uk
+44(0)114 2717959

Key words: miR-145, myofibroblast, CAF, microRNA

Running title: Tumour suppressive functions of mesenchymal miR-145

Summary: Cancer-associated fibroblasts (CAF) contribute to immune evasion, therapy resistance and metastasis of tumours. The presence of myofibroblastic CAF correlates with poor survival, but the mechanisms by which they are generated are poorly understood. Here we identify a microRNA, miR-145, which inhibits and reverses myofibroblast differentiation by acting in a negative feedback loop with transforming growth factor β1. This reveals a novel mechanism underlying myofibroblast and CAF development which may offer therapeutic opportunities.

Abstract

The dissemination of cancer cells to local and distant sites depends on a complex and poorly understood interplay between malignant cells and the cellular and non-cellular components surrounding them, collectively termed the tumour microenvironment. One of the most abundant cell types of the tumour microenvironment is the fibroblast, which becomes corrupted by locally derived cues such as TGF-β1 and acquires an altered, heterogeneous phenotype (cancer-associated fibroblast, CAF) supportive of tumour cell invasion and metastasis. Efforts to develop new treatments targeting the tumour mesenchyme are hampered by a poor understanding of the mechanisms underlying the development of CAF.

Here we examine the contribution of microRNA to the development of experimentally-derived CAF and correlate this with changes observed in CAF derived from tumours. Exposure of primary normal human fibroblasts to TGF-β1 resulted in the acquisition of a myofibroblastic CAF-like phenotype. This was associated with increased expression of miR-145, a miRNA predicted *in silico* to target multiple components of the TGF-β signaling pathway. miR-145 was also over-expressed in CAF derived from oral cancers. Over-expression of miR-145 blocked TGF-β1-induced myofibroblastic differentiation and revert CAF towards a normal fibroblast phenotype.

We conclude that miR-145 is a key regulator of the CAF phenotype, acting in a negative feedback loop to dampen acquisition of myofibroblastic traits, a key feature of CAF associated with poor disease outcome.

Introduction

It is becoming increasingly apparent that interactions between malignant cells and

the cells and other constituents of the tumour microenvironment play a key role in disease outcome (1). Fibroblasts are one of the most numerous cells in the tumour microenvironment and act to modulate both cancer cell behaviour and the host immune responses by remodelling the extracellular matrix (ECM) and secreting a wealth of soluble factors able to interact with nearby cellular receptors via cell autonomous and subservient mechanisms (2). The phenotypes of the fibroblasts surrounding a tumour (collectively termed cancer associated fibroblasts; CAF) are complex and varied, but certain CAF features are strongly associated with cancer cell dissemination and poor outcome (3). The best characterized of these is the presence of 'myofibroblastic' CAF; cells expressing alpha smooth muscle actin (αSMA) which at least superficially resemble myofibroblasts found transiently in healing wounds (4). Myofibroblastic CAF are contractile, secretory cells that generate an altered extracellular matrix and are generally accepted to contribute to an extracellular milieu supportive of cancer cell invasion and metastasis (2). The presence of αSMA-rich CAF is correlated with poor outcome in a number of cancers, suggesting a key role in disease progression (3,5–7). The source of myofibroblastic CAF is controversial but at least some are likely to arise from differentiation (or 'activation') of resting fibroblasts provoked by signals, such as TGF-β1, released from cancer cells and inflammatory cells recruited to the tumour microenvironment (8).

Despite the wealth of data supporting a role for CAF in contributing to tumour metastasis, little is known of the mechanisms underlying CAF development from resident stromal fibroblasts. Here, we applied an *in silico* approach to identify a microRNA, miR-145, found predominantly in mesenchymal cells (9), putatively able to target components of the TGF-β1 signalling pathway. We subsequently examined

the effects of this microRNA on the phenotype of normal fibroblasts, myofibroblasts and CAF. Expression of miR-145 was induced by exposure of normal fibroblasts to TGF-β1 and was also elevated in CAF. Overexpression of miR-145 inhibited and reversed the development of myofibroblastic traits and stromal-epithelial interactions, indicating the existence of a miR-145/TGF-β negative feedback loop in myofibroblasts and CAF. This suggests the possibility of exploiting this therapeutically to reduce pro-tumourigenic traits of stromal fibroblasts.

Materials and methods

Routine tissue culture: All cells were routinely cultured in Dulbecco's modification of Eagle's medium (DMEM), supplemented with 10% (v/v) foetal bovine serum (FBS) and 2 mM L-glutamine, without antibiotics at 37 ℃ with 5% (v/v) CO_2. Primary fibroblasts were used within 3-9 passages. For TGF-β1 treatment, oral fibroblasts were seeded at 250,000 cells per well in a six well plate, allowed to settle before being serum starved for 24 h before treatment with 5 ng/ml TGF-β1 for 24-96 h (as indicated in individual figure legends) in serum free DMEM supplemented with 2 mM L-glutamine.

Primary normal oral fibroblasts (NOF) were isolated from informed consenting patients undergoing wisdom tooth extraction at the Charles Clifford Dental Hospital (Sheffield Research Committee ethics permission 09/H1308/66) (10). CAF were isolated from oral squamous cell carcinoma (OSCC) of consenting patients at the University of Campinas (CAFC) and the University of Glasgow prior to the introduction of current ethical requirements (CAF1-10). CAF2, CAF4, CAF8, CAF9,

and CAF10 were obtained from GU-SCC (genetically unstable-SCC) biopsies known to contain tumourigenic SCC keratinocytes whereas GS-SCC CAF (genetically stable-SCC), CAF1, CAF3, CAF5, CAF6 & CAF7 were obtained from GS-SCC biopsies (11–13), In addition to NOF cultures, normal human oral fibroblast cultures NHOF-1 and NHOF-5 were obtained from the University of Peridanya, Kandy, Sri Lanka (14). Human primary dermal fibroblasts, HDF1 (Promocell) and HDF2 (09/H1308/66)

were kind gifts from Dr Simon Whawell and Prof Sheila MacNeil respectively. H357, a cell line isolated from tongue OSCC (15), was obtained from ATTCC and cell identity was confirmed by satellite tandem repeat (STR) analysis of cells within 10 passages.

The primary fibroblasts used in this study were isolated from separate institutions using adapted protocols. A full table of the cells used in this study and the isolation methods are given in table 1.

Fibroblast isolation: Primary fibroblasts were isolated from oral biopsies as previously described (Hearnden et al., 2009), where the keratinocytes were removed by incubation with 0.1% (w/v) Difco trypsin (BD Biosciences) at 4℃ overnight and subsequently scraped with a scalpel to collect the epithelium. The remaining tissue was finely minced and enzymatically digested with collagenase (0.5% (v/v)) at 37℃ with 5 % (v/v) CO_2 overnight. The collagenase suspension was centrifuged at 2000 rpm for 10 min to retrieve the NOFs. NOFs were initially cultured with routine culture media containing 0.625 µg/ml amphotericin B and 100 i.u./ml penicillin and 100 µg/ml streptomycin, before removing the antibiotics for experimental use.

Alternatively, in the case of fibroblasts provided by Prof E. Ken Parkinson (QMUL,

UK), issue specimens were finely cut, washed with foetal bovine serum and incubated for 30-40 min in a dry atmosphere at 37℃. A small amount of DMEM plus 10 % (v/v) FBS (~ 2 ml) was added to cover the tissue, then the cells were left to grow as explants for 3 days at 37℃. Fibroblasts were selectively cultured in routine culture media (DMEM plus 10% (v/v) FBS and 2mM L-glutamine), where cultures contained keratinocytes, these were removed by the addition of 0.02 % (v/v) EDTA for 30 s, followed by an equal volume of PBS (Stanley et al., (1979) and Prime et al., (1990)).

In the case of fibroblasts provided by Prof R Coletta (University of Campinas, Brazil), tissue samples were washed three times with PBS, finely cut and placed in 1 ml DMEM plus 10 % FCS and antibiotics at 37^{o}C in a humidified atmosphere of 5 % (v/V) CO_2. Cell outgrowth was observed until confluence while changing the media every 2-3 days. Cells were trypsinised and seeded at low densities to isolate individual myofibroblast clones (Sobral et al, 2011).

Transfection: Synthetic oligonucleotide premiRs (premiR-143, premiR-145 or negative premiR; 50 nM) and siRNAs (versican siRNA and negative siRNA; 50 nM) (all Life Technologies) were transiently transfected into the primary oral fibroblasts using Oligofectamine (Life Technologies) in Opti-MEM (Life Technologies). Transfection was performed before or after TGF-β1 treatment. Conditioned media (serum-free DMEM supplemented with 2 mM L-glutamine) were collected after 24 h for subsequent use in transwell migration assays.

Immunocytochemistry: To visualise αSMA stress fibres, 250,000 fibroblasts were

seeded on glass coverslips in six-well plates. After treatments/transfections they were fixed with methanol for 10 min, permeabilised by using 4mM sodium deoxycholate and incubated with a FITC-conjugated anti-human αSMA mouse antibody (clone 1A.4; 1:100; Sigma-Aldrich Cat#F3777, RRID:AB_476977) for 12 h at 4 ℃, following blocking of non-specific binding sites in 2.5% (w/v) bovine serum albumin (BSA) in phosphate buffered saline (PBS) for 30 min. Coverslips were washed twice with PBS, mounted using mounting media containing 4',6-diamidino-2-phenylindole (DAPI; Vectorshield), viewed using a Ziess Axioplan 2 fluorescence light microscope at 40x and imaged using Proplus 7.0.1 image software.

Contractility assay: Fibroblast-populated collagen gels were prepared as previously described (16) using transiently transfected or un-modified normal human primary oral fibroblasts as described in individual figure legends.

Quantitative Real Time PCR: Total RNA was extracted from pelleted fibroblasts using the RNeasy (Qiagen) kit according to the manufacturer's instructions. RNA was quantified using a Nanodrop 1000 spectrophotometer (Thermo). RNA (100 ng) was reverse transcribed using the high capacity cDNA Reverse Transcription kit (Applied Biosystems), according to the manufacturer's protocol. Specific mature microRNAs were reverse transcribed from 10 ng RNA using specific Taqman reverse transcription microRNA probe/primers for mature miR-143, miR-145 and the small nuclear RNA RNU48 as a reference (Applied Biosystems). Total or specific miRNA-derived cDNA was subsequently used as a template for SYBR green or Taqman real time quantitative PCR amplification (7900HT fast Real Time-PCR system, Life Technologies). Sequences of primers used for SYBR analysis (Sigma) were as

follows: U6 Forward (F) 5' CTCGCTTCGGCAGCACA3', U6 Reverse (R) 5'AACGTTCACGAATTTGCGT3', αSMA F 5'GAAGAAGAGGACAGCACTG3', αSMA R 5'TCCCATTCCCACCATCAC3', fibronectin-1 with extra domain A (FN1-EDA) 5'TGGAACCCAGTCCACAGCTATT3', FN1-EDA R 5'GTCTTCTCCTTGGGGGTCACC3', collagen 1A (COL1A1) F 5'GTGGCCATCCAGCTGACC3', COL1A1 R 5'AGTGGTAGGTGATGTTCTGGGAG3' connective tissue growth factor (CTGF) F 5' GGGAAATGCTGCGAGGAGT 3', CTGF R 5'AGGTCTTGGAACAGGCGCTC 3', matrix metalloproteinase 2 (MMP2) F 5' AATAATTCCGCTTCCAGGGCACATCC 3', MMP2 R 5' TTATTGCGGTCGTAGTCCTCAGTGGT 3'. Versican isoform specific Taqman probes (Applied Biosystems) were used to assess the expression of V0 and V1 versican isoform transcripts. Relative expression was calculated using the ΔΔCT method (17) normalised to endogenous controls U6 (SYBR green), or RNU 48 (Taqman). All qPCR was carried out according to best-practice MiQE guidelines (18).

Immunoblotting: Total protein lysates were prepared in radio-immunoprecipitation assay (RIPA) buffer supplemented with complete mini protease inhibitor cocktail (Roche) and benzonuclease (Sigma). Protein lysates (20-30 µg) were resolved by 3-8% (v/v) SDS-polyacrylamide gel (Life Technologies) electrophoresis (SDS-PAGE) in Tris-acetate buffer (Life Technologies). Proteins were transferred onto a nitrocellulose membrane (Millipore) by wet transfer or iBlot dry transfer (Invitrogen), and incubated in blocking solution (5% (w/v) milk powder and 3% (w/v) bovine serum albumin (BSA) in Tris buffered saline (TBS) with 0.05% (v/v) Tween 20 (TBS-T)) for 1 h. Mouse monoclonal anti-human αSMA (clone 1A4; Sigma-Aldrich Cat#A2547,

RRID:AB_476701), goat polyclonal anti-human versican (R&D systems), or monoclonal rabbit anti-human GAPDH (Sigma-Aldrich Cat#G9295, RRID:AB_1078992) antibodies were diluted (1:1000) in blocking solution and incubated with membranes at 4℃ overnight. The membrane was washed 3 x 5 min with TBS-T, and subsequently incubated with a horseradish peroxidase-conjugated (HRP) secondary antibody (1:3000 in blocking solution), for 1 h at ambient temperature. The membrane was washed 3 x 10 min in TBS-T, and developed using enhanced chemiluminescence (Pierce).

Migration and Invasion assays: Conditioned media collected from transfected and TGF-β1 (5 ng/ml) treated fibroblasts were centrifuged at 2,500 x *g* and the supernatant was placed into the bottom of a well of a 24-well plate. H357 cells, previously serum-starved for 24 h, were resuspended into 0.1% (w/v) BSA in DMEM supplemented with L-glutamine (2 mM) and seeded at a density of 100,000 cells/well into the top of a transwell chamber (BD Biosciences). Transwells were coated with Matrigel (300 µg/ml; Corning) to assess cell invasion. Cells were allowed to migrate for 36 h at 37℃ and 5% (v/v) CO_2 in the presence of 1 mg/ml mitomycin C, to inhibit cell proliferation. Transwell chambers were swabbed to remove non-migrated cells in the top of the chamber and fixed in methanol for 10 min. Migrated cells were stained with 0.1% (w/v) crystal violet and imaged at four randomly selected fields of view per transwell at 40x magnification using a light microscope. Migrated cells were then counted using ImageJ.

Statistical analyses: A paired two-tailed student's t-test was used to test for statistical significance. A Mann Whitney U test (performed in GraphPad Prism 6) was used to

assess significance in differential gene expression in NOFs and CAF. All data presented is n=3, unless otherwise stated. N=3 refers to biological replicates from the same fibroblast strain, however each experiment has been repeated in at least 2 strains and a representative figure was selected and shown for conciseness.

Results

TGF-β1 stimulates pro-tumourigenic myofibroblast transdifferentiation

The ability of TGF-β1 to induce myofibroblast transdifferentiation of primary human fibroblasts was examined using several established markers of the myofibroblast phenotype (19–23). Treatment of oral fibroblasts with TGF-β1 (5 ng/ml) resulted in a time-dependent increase in the expression of αSMA, versican (VCAN, V0 isoform) and fibronectin 1 extra domain A (FN1-EDA) transcripts (Fig 1a-c), with a corresponding increase in αSMA protein levels and the appearance of αSMA-rich stress fibres (Fig 1d&e). This was associated with increased ability to contract collagen I lattices (Fig 1f), in keeping with previous reports (22). Conditioned medium from TGF-β-induced myofibroblasts promoted more cancer cell migration and invasion than medium from untreated fibroblasts (Fig 1g&h). It is noteworthy that not all the different cultures of primary fibroblasts tested, obtained from different patients, responded equally to TGF-β1 (Fig S1).

MicroRNA-145 is upregulated during myofibroblast transdifferentiation

In order to begin to examine the molecular mechanisms underlying the TGF-β-induced acquisition of a pro-tumourigenic, myofibroblastic phenotype by primary fibroblasts, we carried out an *in silico* analysis to identify miRNA predicted to target components of the TGF-β1 signalling pathway, using a variety of online algorithms

including DIANA (http://diana.cslab.ece.ntua.gr/). One of the candidate miRNA identified using this approach, miR-145, is predicted or functionally demonstrated in the literature to have numerous targets or putative targets in the TGF-β1 pathway (Fig 2a), and was upregulated in response to TGF-β1 treatment in a number of NOF and CAF (isolated from patients with oral squamous cell carcinomas (14)) cultures analysed (Fig 2b&c) but with heterogeneity in response between different cultures. Having identified a putative role for miR-145 in fibroblast responses to TGF-β1, we next analysed the expression levels of mature miR-145 in a panel of ten NOF and ten CAF miR-145 expression was statistically significantly higher in CAF than in normal oral fibroblasts (Fig 2d).

miR-145 inhibits myofibroblast differentiation in response to TGF-β1

In order to examine the effect of miR-145 on myofibroblast differentiation, a synthetic miRNA functionally mimicking mature miR-145 or a control, non-targeting miRNA, were transfected into primary oral fibroblasts and the effect on markers of the myofibroblastic phenotype was examined. Over-expression of miR-145 (Fig 3a) resulted in an almost complete abolition of the ability of TGF-β1 to induce αSMA transcript levels (Fig 3b) and a reduction of TGF-β-induced αSMA protein levels, as determined by immunoblotting (Fig 3c). No change in the basal level of αSMA was observed in response to miR-145 over-expression in the absence of TGF-β1. Overexpression of miR-143, a miRNA co-expressed with miR-145 as part of a bicistronic cluster (24), resulted in a small decrease in the expression of αSMA transcript but had no effect on αSMA protein levels (Fig 3b&c). In keeping with these findings, we observed a modest, but significant, reduction in the ability of fibroblasts to contract collagen gels in response to TGF-β1 compared to controls (Fig 3d).

Similar results with regards to αSMA expression were obtained using dermal fibroblasts, suggesting the effects of miR-145 are not tissue specific (Fig 3e,f).

We next examined the ability of miR-145 to influence extracellular matrix production, alterations of which are associated with myofibroblastic CAF (19,22,23,25). Heterologous over-expression of miR-145 was found to significantly and markedly decrease the expression of transcripts derived from a number of genes encoding components of the extracellular matrix, including FN1-EDA, connective tissue growth factor (CTGF), COL1A1, MMP2 and both variants of VCAN expressed in oral fibroblasts (VCAN V0 and V1), and to block the upregulation of these genes in response to TGF-β1 (Figure 4a-f). The down-regulation of VCAN was also observed at the protein level, as determined by immunoblotting (Fig 4g) with the level of knockdown approaching that achieved by VCAN-specific siRNA (Fig 4g). Over-expression of miR-143, previously reported to regulate VCAN expression (26), had no effect on either VCAN transcript or protein levels (Fig 4g). Over-expression of miR-145 attenuated the ability of myofibroblasts to stimulate cancer cell migration and invasion in a paracrine manner (Fig 4h&i). Similar effects of miR-145 on the fibroblast phenotype were obtained with dermal fibroblasts (Fig 4j&k).

miR-145 regulates the CAF phenotype

Having established the ability of miR-145 to inhibit the acquisition of a CAF-like myofibroblastic phenotype in normal oral fibroblasts, we next examined its effects in CAF. Over-expression of miR-145 in CAF resulted in a decrease in both basal and TGFβ-induced αSMA, COL1A1 and FN1-EDA transcript levels (Fig 5a-c) and a significant reduction in the ability of TGF-β1 to induce the formation of αSMA-rich stress fibres (Fig 5d). As observed in normal fibroblasts, miR-145 overexpression

was able to inhibit TGF-β-induced αSMA levels in all the CAF cultures analysed (Fig 5e and Fig S2A-C), and reduced both basal and TGF-β-induced VCAN protein expression (Fig 5e). Over-expression of miR-145 in CAF inhibited paracrine stimulation of cancer cell migration in two of the four CAF cultures tested (Fig 5f). Each of the four CAF cultures used had a higher endogenous miR-145 expression relative to average NOF miR-145 levels (Table S1).

To further examine the regulation of CAF phenotype by miR-145 we investigated a possible correlation between miR-145 expression levels and, both endogenous and TGF-β-induced, αSMA gene expression. We found a significant, positive correlation between endogenous miR-145 and αSMA expression in both NOF and CAF cultures (R^2=0.7387, p<0.001; Fig S3a). However, it should be noted, if the fibroblast culture with the highest level of αSMA was omitted from the regression analysis, the correlation was no longer significant (R^2 =0.06846, p= 0.2278). There was also a trend towards a positive correlation (which didn't, however, reach significance) between CAF endogenous miR-145 levels and the magnitude of the TGF-β-induced αSMA (Fig S3b).

miR-145 rescues the CAF phenotype

In order to examine whether these findings would hold therapeutic potential we tested the ability of miR-145 to rescue the CAF phenotype. TGF-β1 treated NOF, which were subsequently transfected with miR-145 mimic, showed markedly reduced expression of CAF markers αSMA, COL1A1 and FN1-EDA (Fig 6a-d) and also a significant reduction in versican V0 and V1 expression (Fig 6e&f). The same reversal of TGF-β1 induced CAF phenotype was seen in dermal fibroblasts (HDF; Fig 6g-l). The extent of miR-145 overexpression was assessed by RT-qPCR in NOFs and

HDFs (Fig S4a&b).

Discussion

The molecular mechanisms underlying the development of CAF from resident stromal fibroblasts are poorly understood, hampering the development of stromally-directed therapies. Here we identify miR-145 as a key regulator of the differentiation of myofibroblastic CAF from resting fibroblasts. We provide evidence that miR-145 levels are elevated in the majority of CAF isolated from oral squamous cell carcinomas compared to normal resting oral fibroblasts, and that induction of a myofibroblastic CAF-like phenotype *in vitro* results in induction of miR-145 expression. Furthermore, we show that miR-145 suppresses cytoskeletal and matricellular markers of myofibroblast activation, and paracrine stimulation of cancer cell migration and invasion, suggesting miR-145 up-regulation may serve to limit pro-tumourigenic, myofibroblastic differentiation in the tumour microenvironment.

Whilst tumour-suppressive effects of miR-145 have been described in both tumour cells and fibroblasts (27–30), two recent studies suggested that miR-145 is restricted to, or at least significantly enriched in, cells of mesenchymal origin (9,31). In keeping with this, functions have been ascribed to miR-145 in a variety of mesenchymal cells, including smooth muscle cells and fibroblasts (32–36). In both of these cell types miR-145 is most commonly described as having the ability to promote differentiation, although a very recent study demonstrated that the effects of miR-145 on the vascular smooth muscle cell (VSMC) phenotype are context-specific, and that miR-145 is able to inhibit responses to TGF-β1, limiting the differentiation of VSMCs (36). This is consistent with our findings, in which we observe miR-145 levels to increase in response to TGF-β1 but to down-regulate numerous target genes induced by TGF-

β1, thereby inhibiting the development of a myofibroblastic phenotype. In contrast to other studies (33–35), however, we found no evidence of miR-145 having the ability to induce myofibroblast markers in the absence of TGF-β1; indeed in tumour-derived CAF, miR-145 reproducibly reduced the basal levels of both cytoskeletal and matricellular myofibroblast markers. These conflicting results may be the result of species differences or the use of embryonic versus adult fibroblasts, but also suggests a degree of complexity characteristic of mechanisms regulating the actions of TGF-β1, likely reflecting the need to tune responses to the dynamic tissue microenvironment. It is noteworthy that our *in silico* analysis and unpublished data (de Oliveira et al, data not shown) indicates that miR-145 may target the receptors and signaling components of other TGF-β1-related molecules, including activin A and bone morphogenetic proteins (BMPs), suggesting miR-145 may play a role in regulating cellular responses to these stimuli in addition to TGF-β1; we speculate that this pleiotropy may contribute to the complex and contradictory functions reported for miR-145 in fibroblasts and smooth muscle cells.

TGF-β1 signalling within stromal fibroblasts plays a crucial role in determining fibroblast responses to local cues such as ECM remodeling, and as such is subject to multiple layers of regulation (reviewed in (37)). Dysregulation of the TGF-β1 pathway, such as TGF-β1 overexpression and loss of function of TGFβ receptor II (TGF-βRII) in fibroblasts, promotes tumourigenesis in adjacent epithelial cells and malignant progression (38–40). A variety of mechanisms exist to regulate TGF-β1 signalling, including negative feedback, exemplified by the role of SMAD7, which is induced by TGF-β1 but limits its downstream effects by negatively regulating the canonical signaling pathway via SMAD3/4 (41). Our data suggests miR-145 function in a similar manner by negatively regulating the responses of stromal fibroblasts to

TGF-β1.

Myofibroblastic differentiation is a complex process regulated by both intrinsic and extrinsic cues. Among extrinsic cues, the ECM plays a prominent role, both through interaction of cells with individual components and by mechanical forces imposed by the ECM. In this study, we provide evidence that miR-145 reduces the synthesis of a variety of ECM components in the presence and absence of TGF-β1. What is yet to be determined, however, is whether these are direct or indirect targets of miR-145. Of those targets studied, only CTGF is reported to be directly targeted by miR-145 (42); we are currently seeking to validate this in primary fibroblasts. miR-145 has several documented targets in the TGF-β pathway including SMAD3 (43) and TGF-βRII (36), down-regulation of which may influence the production of ECM components. We propose that miR-145 regulates responses to TGF-β1 by targeting multiple components of the pathway, possibly differentially in response to yet undetermined additional context-specific cues. In the tumour microenvironment, this confers on miR-145 the ability to reduce the myofibroblastic, pro-tumourigenic CAF phenotype.

Here we have outlined a key role for mesenchymal miR-145 in a TGF-β1 feedback loop in stromal fibroblasts. Up-regulated by TGF-β1, miR-145 is able to dampen TGF-β1 mediated myofibroblast transdifferentiation and consequential pro-tumourigenic effects in fibroblasts. This raises the possibility that miR-145 could be exogenously targeted to the tumour microenvironment to attenuate the pro-tumourigenic myofibroblastic phenotype of CAF. It may also hold promise in other contexts in which myofibroblasts play a role, such as fibrotic disorders. miRNA-mediated therapies are currently in clinical trials (reviewed in (44)) and recent developments in miRNA delivery techniques have realised the possibility of

specifically delivering miRNAs to specific tissue microenvironments (45).

Author contributions

GEM, SAF, SAA, PP, EEH, HC and SH conducted experiments. GEM and DWL formulated experimental approach, with input from JWFC, DJB, IP, GJT, SSP, EKP, MM and RDC. MM, RDC, GJT, IP and RDC provided cells or other reagents. DWL and GEM wrote the manuscript. All authors read and had the opportunity to comment on the manuscript.

Conflict of interest statement

The authors declare no conflicts of interest.

Acknowledgements

We acknowledge the financial support of the University of Sheffield, UK. EEH, GEM and HC were the recipients of University of Sheffield Scholarships, EEH and GEM the recipients of Santander Research Mobility Awards, and DWL the recipient of a Newton Fund/FAPESP Travel Award. ICP is supported by a University of Malaya Frontier Research Grant (FG001-17AFR).

References

1. Perez-Moreno, M. When neighbourhood matters: tumour microenvironment. *Clin. Transl. Oncol.*, **11**, 70–74.
2. Cirri, P. *et al.* Cancer-associated-fibroblasts and tumour cells: A diabolic liaison driving cancer progression. *Cancer Metastasis Rev.*, **31**, 195–208.
3. Marsh, D. *et al.* (2011) Stromal features are predictive of disease mortality in oral cancer patients. *J. Pathol.*, **223**, 470–81.
4. Lewis, M.P. *et al.* (2004) Tumour-derived TGF-beta1 modulates myofibroblast differentiation and promotes HGF/SF-dependent invasion of squamous

carcinoma cells. *Br. J. Cancer*, **90**, 822–32.

5. Kellermann, M.G. *et al.* (2007) Myofibroblasts in the stroma of oral squamous cell carcinoma are associated with poor prognosis. *Histopathology*, **51**, 849–53.
6. Tsujino, T. *et al.* (2007) Stromal Myofibroblasts Predict Disease Recurrence for Colorectal Cancer. *Clin. Cancer Res.*, **13**, 2082–2090.
7. Surowiak, P. *et al.* (2007) Occurrence of stromal myofibroblasts in the invasive ductal breast cancer tissue is an unfavourable prognostic factor. *Anticancer Res.*, **27**, 2917–24.
8. Anderberg, C. *et al.* (2009) On the origin of cancer-associated fibroblasts. *Cell Cycle*, **8**, 1461–1462.
9. Chivukula, R.R. *et al.* (2014) An essential mesenchymal function for miR-143/145 in intestinal epithelial regeneration. *Cell*, **157**, 1104–16.
10. Hearnden, V. *et al.* (2009) Diffusion studies of nanometer polymersomes across tissue engineered human oral mucosa. *Pharm. Res.*, **26**, 1718–28.
11. Edington, K.G. *et al.* (1995) Cellular immortality: a late event in the progression of human squamous cell carcinoma of the head and neck associated with p53 alteration and a high frequency of allele loss. *Mol. Carcinog.*,
12. Lim, K.P. *et al.* (2011) Fibroblast gene expression profile reflects the stage of tumour progression in oral squamous cell carcinoma. *J. Pathol.*, DOI: 10.1002/path.2841.
13. Hassona, Y. *et al.* (2013) Progression of genotype-specific oral cancer leads to senescence of cancer-associated fibroblasts and is mediated by oxidative stress and TGF-β. *Carcinogenesis*, DOI: 10.1093/carcin/bgt035.
14. Lim, K.P. *et al.* (2011) Fibroblast gene expression profile reflects the stage of tumour progression in oral squamous cell carcinoma. *J. Pathol.*, **223**, 459–469.
15. Prime, S.S. *et al.* (1990) The behaviour of human oral squamous cell carcinoma in cell culture. *J. Pathol.*, DOI: 10.1002/path.1711600313.
16. Hinsley, E.E. *et al.* (2012) Endothelin-1 stimulates oral fibroblasts to promote oral cancer invasion. *Life Sci.*, **91**, 557–61.
17. Livak, K.J. *et al.* (2001) Analysis of relative gene expression data using real-time quantitative PCR and the 2(-Delta Delta C(T)) Method. *Methods*, **25**, 402–8.
18. Bustin, S. *et al.* (2009) The MIQE guidelines: minimum information for publication of quantitative real-time PCR experiments. *Clin. Chem.*, **55**, 611–22.
19. Hattori, N. *et al.* (2011) Pericellular versican regulates the fibroblast-myofibroblast transition: a role for ADAMTS5 protease-mediated proteolysis. *J. Biol. Chem.*, **286**, 34298–310.

20. Hinz, B. (2007) Formation and function of the myofibroblast during tissue repair. *J. Invest. Dermatol.*, **127**, 526–37.

21. Yeung, T.-L. *et al.* (2013) TGF-β modulates ovarian cancer invasion by upregulating CAF-derived versican in the tumor microenvironment. *Cancer Res.*, **73**, 5016–28.

22. Hassona, Y. *et al.* (2014) Senescent cancer-associated fibroblasts secrete active MMP-2 that promotes keratinocyte dis-cohesion and invasion. *Br. J. Cancer*, **111**, 1230–7.

23. Garrett, Q. *et al.* (2004) Involvement of CTGF in TGF-beta1-stimulation of myofibroblast differentiation and collagen matrix contraction in the presence of mechanical stress. *Invest. Ophthalmol. Vis. Sci.*, **45**, 1109–16.

24. Xin, M. *et al.* (2009) MicroRNAs miR-143 and miR-145 modulate cytoskeletal dynamics and responsiveness of smooth muscle cells to injury. *Genes Dev.*, **23**, 2166–78.

25. Hinz, B. *et al.* (2007) The myofibroblast: one function, multiple origins. *Am. J. Pathol.*, **170**, 1807–16.

26. Wang, X. *et al.* (2010) Repression of versican expression by microRNA-143. *J. Biol. Chem.*, **285**, 23241–50.

27. Pal, A. *et al.* (2013) Cigarette smoke condensate promotes pro-tumourigenic stromal-epithelial interactions by suppressing miR-145. *J. Oral Pathol. Med.*, **42**, 309–14.

28. Sachdeva, M. *et al.* (2010) miR-145-mediated suppression of cell growth, invasion and metastasis. *Am. J. Transl. Res.*, **2**, 170–80.

29. Rani, S.B. *et al.* (2013) MiR-145 functions as a tumor-suppressive RNA by targeting Sox9 and adducin 3 in human glioma cells. *Neuro. Oncol.*, **15**, 1302–16.

30. Bufalino, A. *et al.* (2015) Low miR-143/miR-145 Cluster Levels Induce Activin A Overexpression in Oral Squamous Cell Carcinomas, Which Contributes to Poor Prognosis. *PLoS One*, **10**, e0136599.

31. Kent, O.A. *et al.* (2014) Lessons from miR-143/145: the importance of cell-type localization of miRNAs. *Nucleic Acids Res.*, **42**, 7528–38.

32. Cordes, K.R. *et al.* (2009) miR-145 and miR-143 regulate smooth muscle cell fate and plasticity. *Nature*, **460**, 705–10.

33. Wang, Y.-S. *et al.* (2014) Role of miR-145 in cardiac myofibroblast differentiation. *J. Mol. Cell. Cardiol.*, **66**, 94–105.

34. Yang, S. *et al.* (2013) miR-145 regulates myofibroblast differentiation and lung fibrosis. *FASEB J.*, **27**, 2382–91.

35. Gras, C. *et al.* miR-145 contributes to hypertrophic scarring of the skin by inducing myofibroblast activity. *Mol. Med.*, **21**, 296–304.

36. Zhao, N. *et al.* (2015) MicroRNA miR145 regulates TGFBR2 expression and matrix synthesis in vascular smooth muscle cells. *Circ. Res.*, **116**, 23–34.

37. Papageorgis, P., Stylianopoulos, T. (2015) Role of TGFβ in regulation of the tumor microenvironment and drug delivery. *Int. J. Oncol.* , **46**, 933–43.

38. Kuperwasser, C. *et al.* (2004) Reconstruction of functionally normal and malignant human breast tissues in mice. *Proc. Natl. Acad. Sci. U. S. A.*, **101**, 4966–71.

39. Bhowmick, N.A. *et al.* (2004) TGF-beta signaling in fibroblasts modulates the oncogenic potential of adjacent epithelia. *Science*, **303**, 848–51.

40. Forrester, E. *et al.* (2005) Effect of conditional knockout of the type II TGF-beta receptor gene in mammary epithelia on mammary gland development and polyomavirus middle T antigen induced tumor formation and metastasis. *Cancer Res.*, **65**, 2296–302.

41. Yan, X. *et al.* (2009) Regulation of TGF-β signaling by Smad7. *Acta Biochim. Biophys. Sin. (Shanghai).*, **41**, 263–272.

42. Lee, H.K. *et al.* (2013) MicroRNA-145 is downregulated in glial tumors and regulates glioma cell migration by targeting connective tissue growth factor. *PLoS One*, **8**, e54652.

43. Megiorni, F. *et al.* (2013) Elevated levels of miR-145 correlate with SMAD3 down-regulation in cystic fibrosis patients. *J. Cyst. Fibros.*, **12**, 797–802.

44. Ling, H. *et al.* (2013) MicroRNAs and other non-coding RNAs as targets for anticancer drug development. *Nat. Rev. Drug Discov.*, **12**, 847–865.

45. Cheng, C.J. *et al.* (2014) MicroRNA silencing for cancer therapy targeted to the tumour microenvironment. *Nature*, **518**, 107–10.

Figure legends

Figure 1. TGF-β1 induces myofibroblastic features in primary human fibroblasts. Primary fibroblasts (a-c: NOF2, d: NOF3, e-f: NOF2, g-i: NOF1) were treated with TGF-β1 (5 ng/ml) or serum free DMEM for 24-96 h as indicated. RNA was extracted, reverse transcribed and subjected to qPCR to determine the transcript levels of αSMA (a), VCAN V0 (b) or FN1-EDA (c). Total cell lysates were prepared and immunoblotted for αSMA (d). Following treatment with TGF-β1 for 48 h, cells were fixed in methanol and αSMA visualized using a FITC-conjugated anti-αSMA antibody (e). The ability of fibroblasts treated with TGF-β1 for 48 h to contract collagen 1 was examined compared to serum free DMEM treated controls (f).

Conditioned medium collected from cells exposed to TGF-β1 for 48 h was used in a transwell assay to assess the migration (g) or invasion through Matrigel (h) of H357 cancer cells. ****p<0.0001, ***p<0.001, **p<0.01 assessed using a paired, two tailed student's t-test. n=3, biological replicates in fibroblast strain indicated above.

Figure 2. miR-145 has multiple putative targets in TGF-β signaling pathways and is up-regulated by TGF-β1. Analysis of potential targets of miR-145 using DIANA reveals a number of putative targets in the TGF-β1 signalling pathway as well as other genes associated with myofibroblast differentiation (a). NOF (NOF1-4) were serum starved for 24 h before being exposed to TGF-β1 (5 ng/mL) or vehicle for 24 h. Levels of miR-145 were analysed by conventional qPCR in 10 independent NOF cultures (NOF1-10) (c) and 4 independent CAF cultures (CAF1-10) (c). ****p<0.0001, ***p<0.001, **p<0.01 (b,c) using a paired, two tailed student's t-test, and a Mann Whitney U test (c). N=3, biological replicates (b).

Figure 3. miR-145 overexpression inhibits myofibroblast differentiation. Proliferating NOF (NOF1) were transfected with 50 nM synthetic premiR-143, premiR-145 or a control, non-targeting premiR (negative premiR), incubated for 24 h before being exposed to TGF-β1 (5 ng/mL) or serum free DMEM control for a further 48 h. RNA was extracted and resulting cDNA subjected to qPCR for mature miR-145 (a) or αSMA (b). Total cellular lysate protein from cells transfected as described was immunoblotted for αSMA (c); additionally transfected cells (NOF2-4; data combined) were seeded into collagen I gels and their ability to contract the gels in following treatment with TGF-β1 (5 ng/mL) or vehicle control for 48 h determined (d). Human dermal primary fibroblasts (HDF) were transfected with miR-145 and treated with

TGF-β1, as above. αSMA transcript levels were assessed by qPCR (e) and protein by immunoblotting (f) ****p<0.0001, ***p<0.001, **p<0.01 using a paired, two tailed student's t-test. All n=3, biological replicates in fibroblast strain indicated above.

.

Figure 4. miR-145 alters ECM deposition by fibroblasts. Proliferating NOF ((a-f): NOF1, (g): NOF4, (h-i): NOF1) were transfected with 50 nM synthetic premiR-145 or a control, non-targeting premiR (negative premiR), incubated for 24 h before being exposed to TGF-β1 (5 ng/mL) or serum free DMEM control for a further 48 h. RNA was extracted and resulting cDNA subjected to qPCR for FN1-EDA (A), CTGF (B), COL1A1 (C), MMP2 (D), and VCAN transcripts V0 and V1 (E, F). Total cellular lysate proteins from cells transfected as described, or transfected for 24 h prior to TGF-β1 treatment with either miR-145 or a non-targeting miRNA, siRNA targeting VCAN or a non-targetting siRNA, were immunoblotted for VCAN and reprobed for β-actin as a loading control (G). Conditioned medium was collected after 24 h incubation from NOF transfected as described and treated with TGF-β1 for 48 h. The media was changed for fresh low serum medium before conditioned medium was added to the lower chamber of a transwell assay, and H357 cells in reduced serum medium added to the top of the insert. Cells migrating across the insert were counted (H). The same procedure was followed with matrigel present in the insert (I). Human dermal primary fibroblasts (HDF) were transfected with miR-145 and treated with TGF-β1, as above. FN-EDA1 transcript levels were assessed by qPCR (J) and versican protein by immunoblotting (K). ****p<0.0001, ***p<0.001, **p<0.01 using a paired, two tailed student's t-test. All n=3, biological replicates in fibroblast strain indicated above.

Figure 5. miR-145 regulates the CAF phenotype. Proliferating CAF (CAF1) were transfected with 50 nM synthetic premiR-145 or a control, non-targeting premiR (negative premiR), incubated for 24 h before being exposed to TGF-β1 (5 ng/mL) or serum free DMEM control for a further 48 h. RNA was extracted and resulting cDNA subjected to qPCR for αSMA (A), COL1A1 (B) and FN1-EDA (C). Following treatment with TGF-β1 for 48 h, CAF were fixed in methanol and αSMA visualized using a FITC-conjugated anti-αSMA antibody (D), or total cell lysates were prepared and immunoblotted for αSMA and VCAN; β-actin served as a loading control (E). 4 CAF cultures (CAF1-3, CAFC)) were transfected with miR-145 mimic or non-targeting control and conditioned medium collected before being added to the lower chamber of a transwell assay, and H357 cells in reduced serum medium added to the top of the insert (schematic, F). Cells migrating across the insert were counted . ****p<0.0001, ***p<0.001, **p<0.01 using a paired, two tailed student's t-test. All n=3, biological replicates in fibroblast strain indicated above, except (f) where each the migration assay for each CAF was performed twice.

Figure 6. miR-145 rescues CAF phenotype. Proliferating NOF (NOF2; A-F) and HDF (G-L) were treated with TGF-β1 (5ng/mL) for 48 h and subsequently transfected with 50 nM synthetic premiR-145 or a control, non-targeting premiR (negative premiR), incubated for a further 24 h. RNA was extracted and resulting cDNA subjected to qPCR for αSMA (A and G), COL1A1 (G and I), FN1-EDA (D and J) versican V0 (E and K) and versican V1 (F and L). Following treatment and transfection, total protein lysates were prepared from NOF and HDF, and an immunoblotted for αSMA, with a β-actin loading control (B and H). ****p<0.0001, ***p<0.001, **p<0.01 using a paired, two tailed student's t-test. All n=3, biological replicates in fibroblast strain indicated above, except (f) where each the migration assay for each CAF was performed twice.

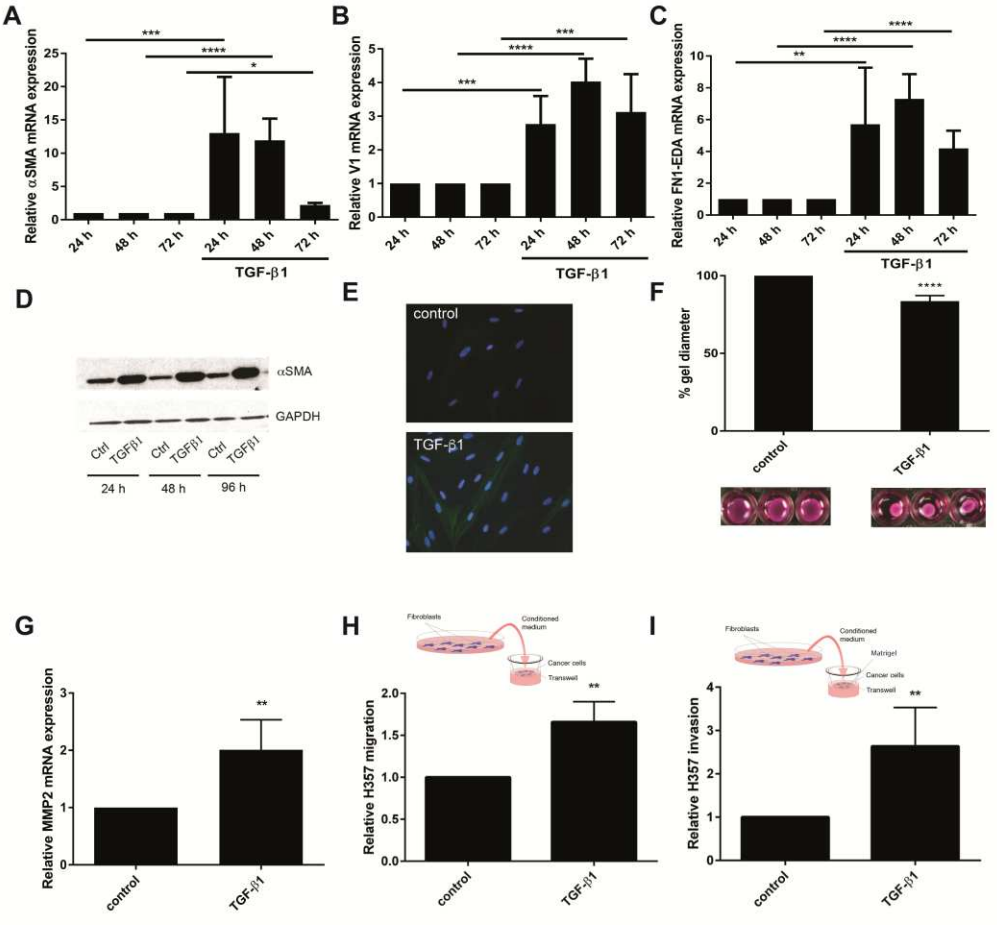

Figure 1

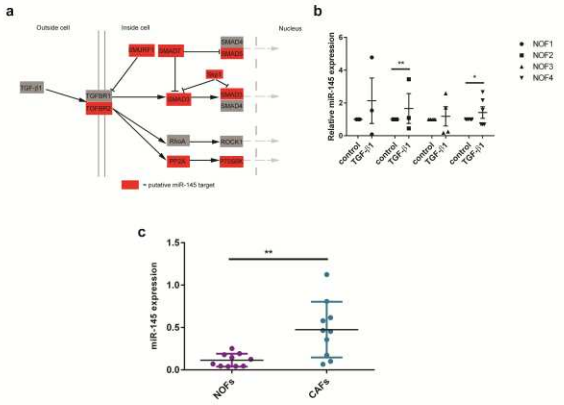

Figure 2

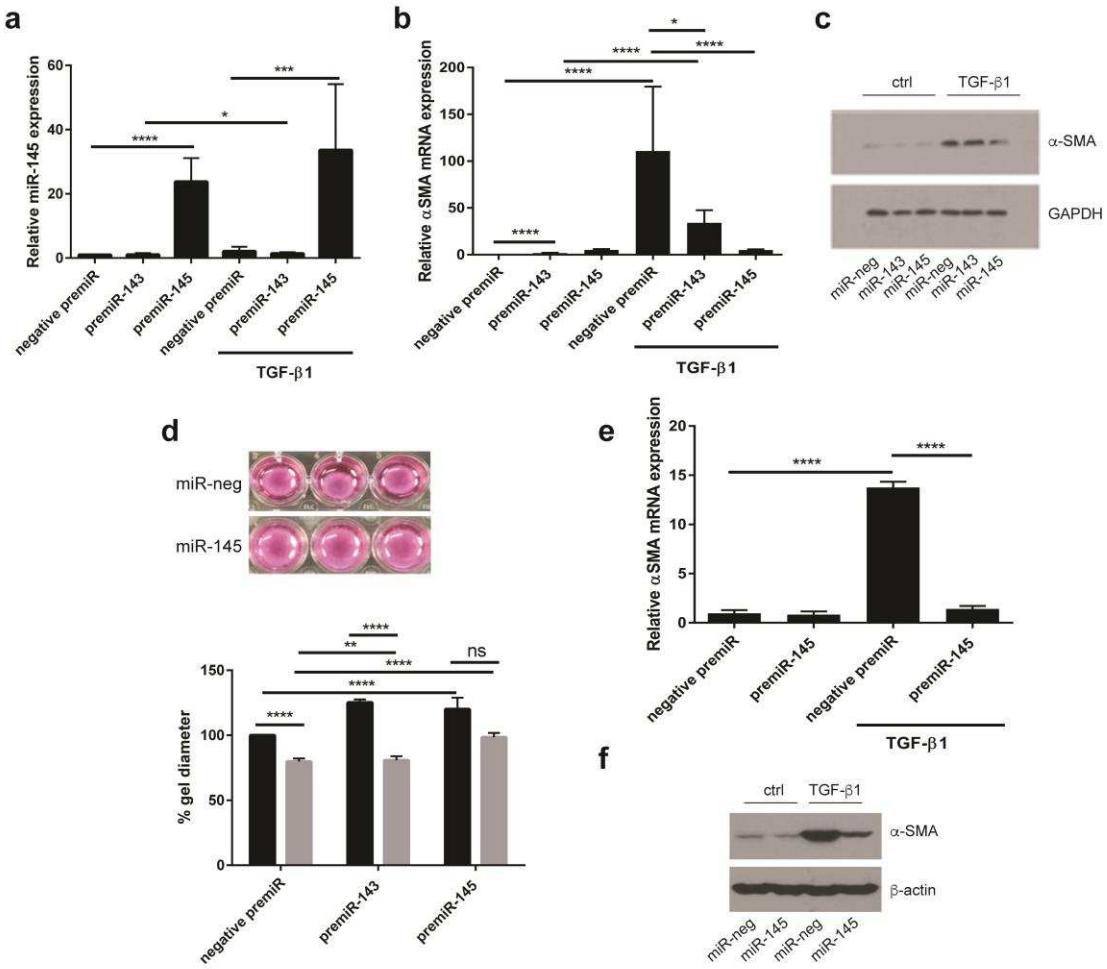

Figure 3

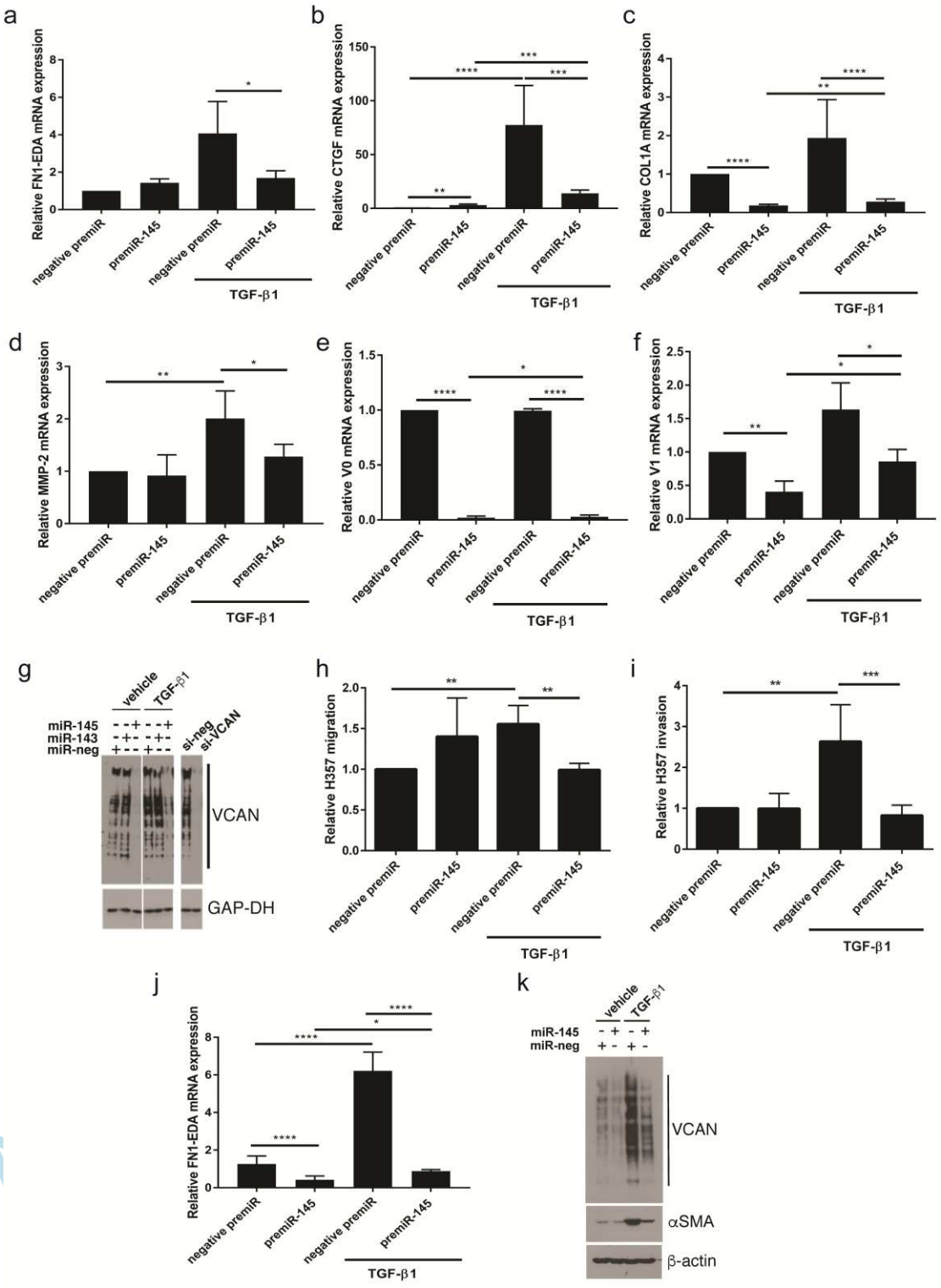

Figure 4

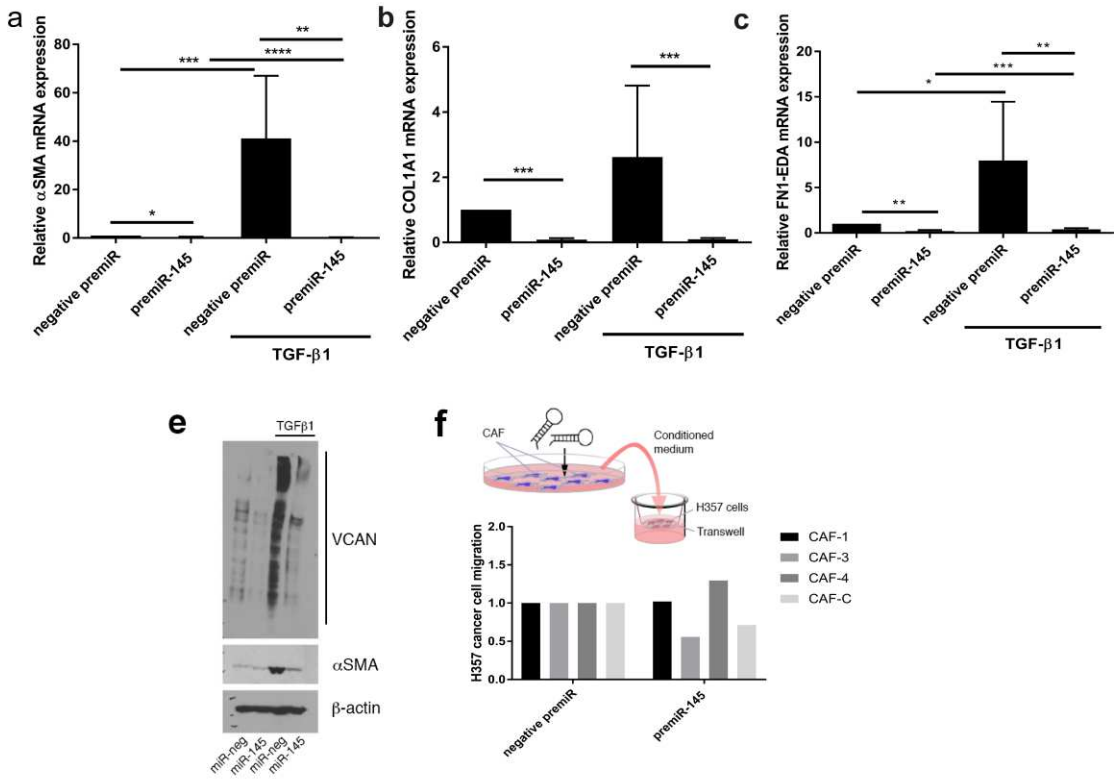

Figure 5

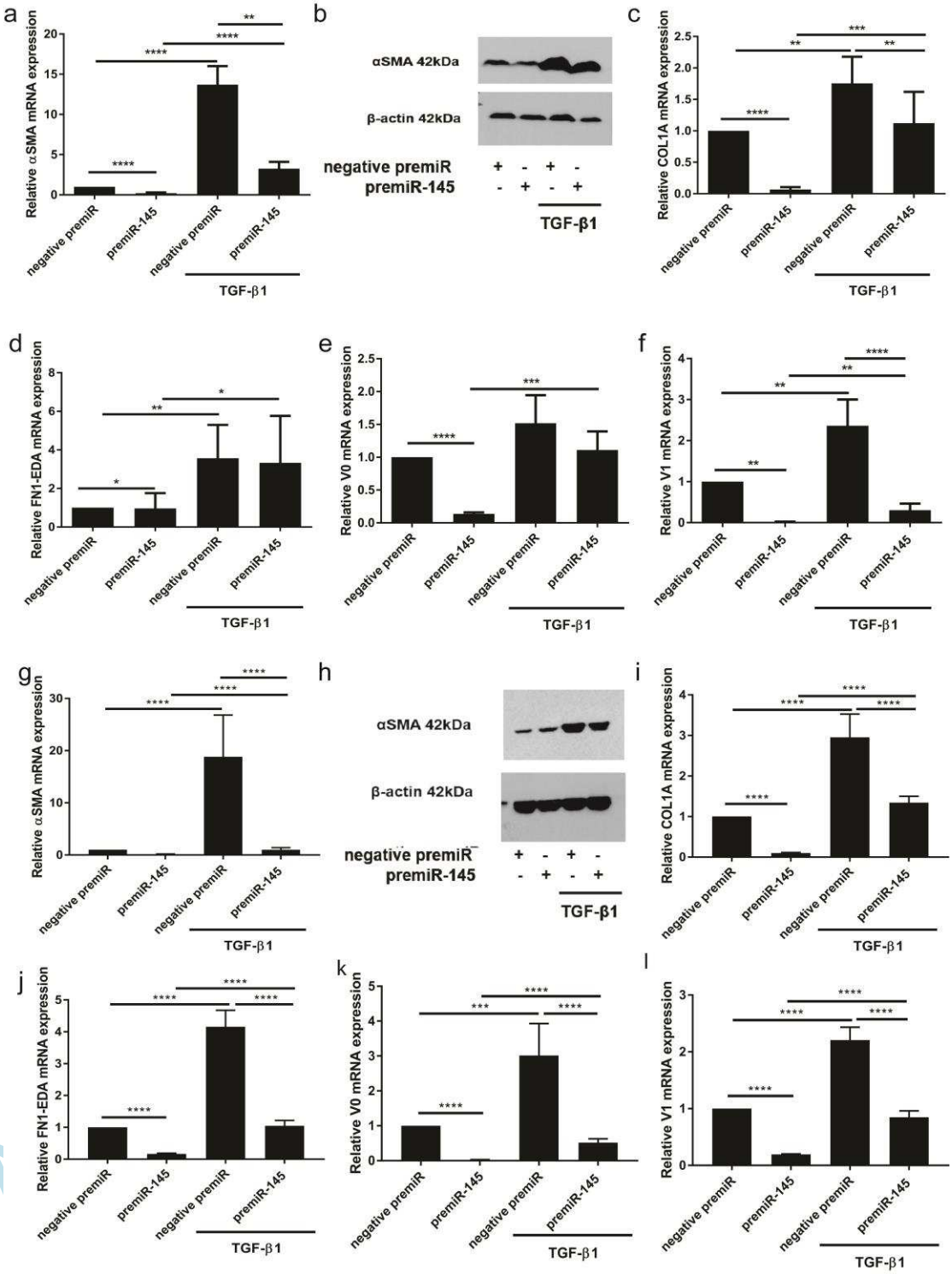

Figure 6